Journal of Theoretical and Applied Mechanics, Sofia, Vol.52 (2022) pp. 248-276
INTERDISCIPLINARY TOPICS

ON THE MECHANICAL BEHAVIOR OF MASONRY WALLS: AN OVERVIEW OF MODELS, SIMULATIONS, EXPERIMENTS AND CODE REGULATIONS

GEORGE I. PAPADOPOULOS, GEORGE D. MANOLIS*

Laboratory for Experimental Mechanics, Department of Civil Engineering, Aristotle University, 54124 Thessaloniki, Greece

[Received: 18 September 2021. Accepted: 05 April 2022]

doi: https://doi.org/10.55787/jtams.22.52.3.248

ABSTRACT: This paper is an overview of the mechanical behavior of masonry walls, which encompasses their response to external loads and their modes of failure as derived from experimental evidence. This material is augmented with numerical modelling techniques and brought into better perspective by examining building code regulations. Furthermore, some key experiments that were performed in the recent past are discussed and the experimental results produced are critically presented, since they are essential for calibrating numerical models and for drafting code regulations.

KEY WORDS: masonry walls, structural mechanics, failure modes, numerical modelling, experimental evaluation, code regulations.

1 INTRODUCTION

Masonry is one of the most ancient building materials and masonry construction techniques have changed little over the millennia. However, knowledge on the mechanical behavior and the overall response of masonry structures to external loads is still rather limited. This contradiction can be explained according to the following reasons, see [1]: (a) The evolution of mechanics occurred simultaneously with the appearance of new and durable materials such as steel and reinforced concrete that reduced the cost of building new structures, which gradually led to a secondary role for masonry use in new buildings; (b) Masonry shows limited stiffness and is characterized by very brittle behavior. As a consequence, the construction cost of various masonry elements increases with height, while at the same time, the number of floors in buildings has to be limited, especially in areas of high seismicity; (c) Masonry exhibits strong anisotropy, as it comprises bricks, mortar and even roughly hewn stones. The diversity of these material is quite spectacular, as are the various

*Corresponding author e-mail: gdm@civil.auth.gr

building techniques used. For these reasons, it becomes clear that one has to explore the basics of the mechanical interaction between the masonry constituents in order to understand the overall behavior of masonry construction.

The design of masonry structures with bearing walls was carried out empirically until the beginnings of the last century. Even in countries with a tradition in in masonry construction, albeit in the absence of any seismicity such as the United Kingdom, multi-story masonry buildings are still being routinely constructed without consideration of transient types of loading. In recent years, however, there is considerable interest world-wide in protecting historical monuments, which are predominantly masonry structures. As a consequence, scientific research on masonry has increased spectacularly and certain advantages have come to the forefront, e.g., soundproofing, fireproofing, material strength and superiority of the external appearance. In sum, the design of masonry buildings in the European Union is carried out according to [2], with the most important part being Part 1-1. This normative frame is being complemented with [3] that focuses on seismic loads, and specifically Chapter 9, which explicitly refers to masonry structures.

2 Mechanical Behavior of Masonry Construction

As mentioned above, the mechanical behavior of masonry construction is characterized by the following:

(a) high compressive strength;

(b) very low tensile strength;

(c) adequate shear strength; and

(d) high degree of anisotropy.

Except for the high compressive strength of masonry, the remaining properties are considered as structural weaknesses. These weak points are not only due to the brittle behavior of the stone-brick-mortar composite, but also on the mechanical behavior of the contact area along the continuous horizontal joints.

2.1 Masonry compressive strength

As mentioned, the compressive strength of masonry is much higher compared to its other mechanical characteristics, and this is the reason why masonry is mainly used as a compressive stress carrying element in a structure. Both strength and failure mechanisms of masonry elements are highly influenced by the angle the compressive force forms with respect to the horizontal joints. More specifically, masonry walls under compression acting vertically to the horizontal joints, fail primarily through

diagonal fracture of the stones/bricks. This is because of tensile stresses that build up in the transverse direction to counterbalance the large transverse deformations of the mortar, as compared to the much smaller ones that develop in the stones/bricks. This results in a constriction of the mortar as $E_m < E_b$, $\nu_m > \nu_b$, where $E\nu$ respectively are the modulus of elasticity and Poisson's ratio of the mortar (subscript m) and of the bricks/stones (subscript b) Thus, under uniaxial compressive loading of the masonry, the stone/brick/mortar composite is in a state of triaxial loading.

2.2 MASONRY TENSILE STRENGTH

The tensile strength of masonry is much lower compared to the compressive one. It varies strongly, depending primarily on the angle traced between the tensile force and the horizontal joints, which is a manifestation of anisotropy. Also, tensile strength values are very scattered, which denotes uncertainty in the values of material parameters. The tensile strength of masonry is influenced by the following factors:

(a) strength of the mortar against detachment (f_{jt});

(b) tensile strength of the mortar (f_{mt}); and

(c) cohesion between mortar and stone/brick (f_{js0}).

Finally, a distinction is made between the tensile strength parallel (f_{wt}^{p}) and normal (f_{wt}^{n}) to the horizontal joints, with the former being much larger in value compared to the latter.

2.3 MASONRY SHEAR STRENGTH

Under realistic loading conditions, no state of pure shear can materialize in the masonry. More specifically, in the plane of the joints not only shear stresses (τ) develop, but also normal stresses (σ_n), even under the self-weight of the masonry itself. The envelope of masonry failure modes that forms under combined loading $(\tau,\ \sigma_n)$ is a very useful tool in earthquake-resistant design, see Fig. 1. Closer examination of these failure envelopes reveals the following points summarized below:

(a) Low values of σ_n (field I), with failure is either due to friction and sliding of the horizontal joint or to stair-shaped sliding of the butt joint and of the horizontal joints. This is often the failure mode of shear-loaded walls, and the linear failure criterion of Coulomb applies as $\tau_u = f_{ws} = f_{ws0} + \mu\sigma_n$, with σ_n considered positive.

(b) Intermediate values of σ_n (field II), with failure due to diagonal cracks that even cross through the stone-brick continuum.

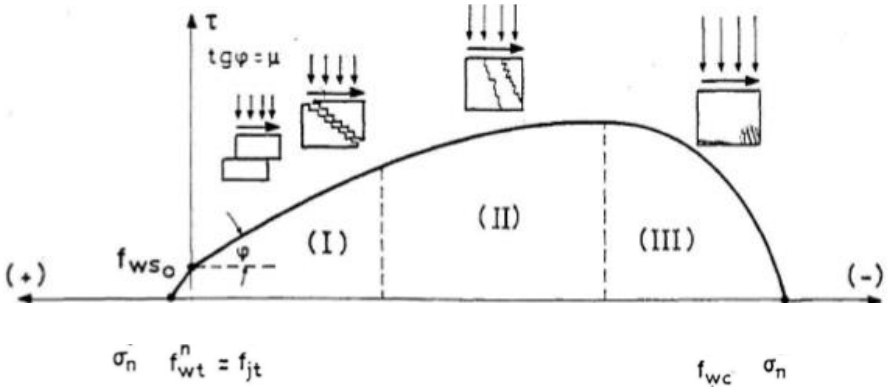

Fig. 1: Typical form of the envelope of masonry failure modes [4].

(c) Higher values of σ_n (field III), with failure of the compressed corner.

(d) Normal tensile stress σ_n axis: The envelope seen in Fig. 1 is almost a straight line in the left-hand side area with a distinctive inclination, and in most cases $f_{ws0} > f_{jt}$.

In general, the failure envelope is strongly influenced by the mechanical properties of the stones, mortar and joints, and even by the shape of the stones. For the initial part of the envelope that is nearly linear, the values of friction coefficient are within the range of $0.4 \leq \mu \leq 0.7$ according to the literature. This is the most important area, because it corresponds to typical normal stresses in masonry under operating conditions.

3 Failure Mechanisms of Masonry Structures

In what follows, we depict the failure mechanisms that develop in masonry walls, followed by material on bearing joint failure.

3.1 Failure mechanisms under cyclic loading for single story buildings

In Fig. 2, typical failure mechanisms for single story buildings under transverse load are presented [4]. We observe that in cases (a) and (b), there is no diaphragm or perimetric beam and as a result, there is no connection between the walls. Thus, following detachment, each wall behaves as a single entity. In this case, out of plane bending is critical for the walls that are perpendicular to the direction of the seismic motion. In case (c), there is a perimetric beam but no diaphragm on the masonry crown and detachment of the walls from each other at the corners is prevented. However, due to the

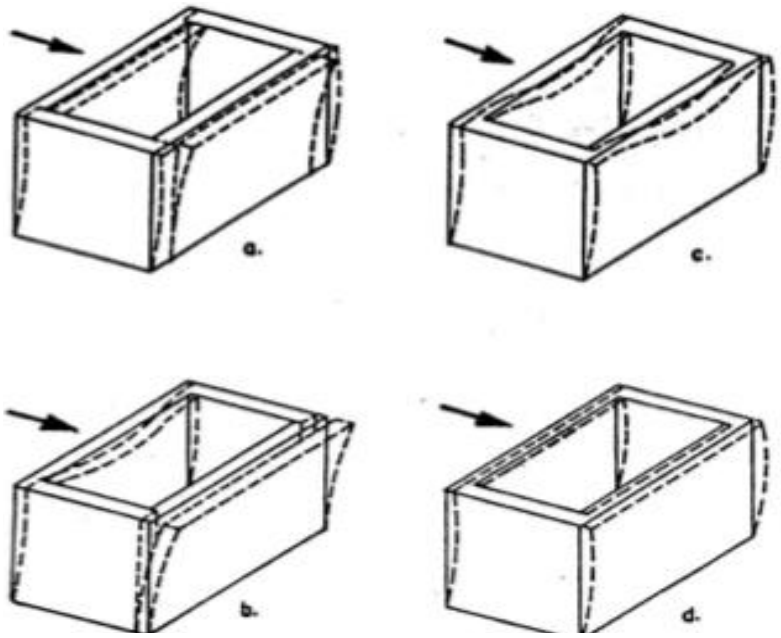

Fig. 2: Typical failure mechanisms for one story buildings under transverse load [4].

small bending stiffness of the perimetric beam transverse to the plane, a pronounced bending outside the plane of the walls perpendicular to the direction of the earthquake motion can no longer be prevented. Finally, in case (d), there is a complete diaphragm action at the level of the masonry crown. This ensures the transmission and subsequent absorption of the entire horizontal force exerted by the earthquake, from the walls that lie in its direction. Thus, masonry walls act as a high-strength discs.

Based on this type of behavior of a single-story building, we distinguish between the following failure mechanisms for a single wall or a pillar, see Fig. 3:

(a) A single cantilevered wall is very weak when earthquake-induced forces are perpendicular to its plane (Fig. 3a). Then, the forces of inertia are resisted by its self-weight, with negligible bending stiffness of the base cross-section.

(b) A single cantilevered wall loaded in its plane shows a substantial amount of resistance because it behaves as a disc i.e., it is actually a shear wall. The failure mode in this case depends on the geometry, the ratio of the vertical to horizontal loads and the mechanical properties of the masonry. More specifically, we have: (i) Sliding or pure shear failure along a horizontal joint (Fig. 3b); (ii)

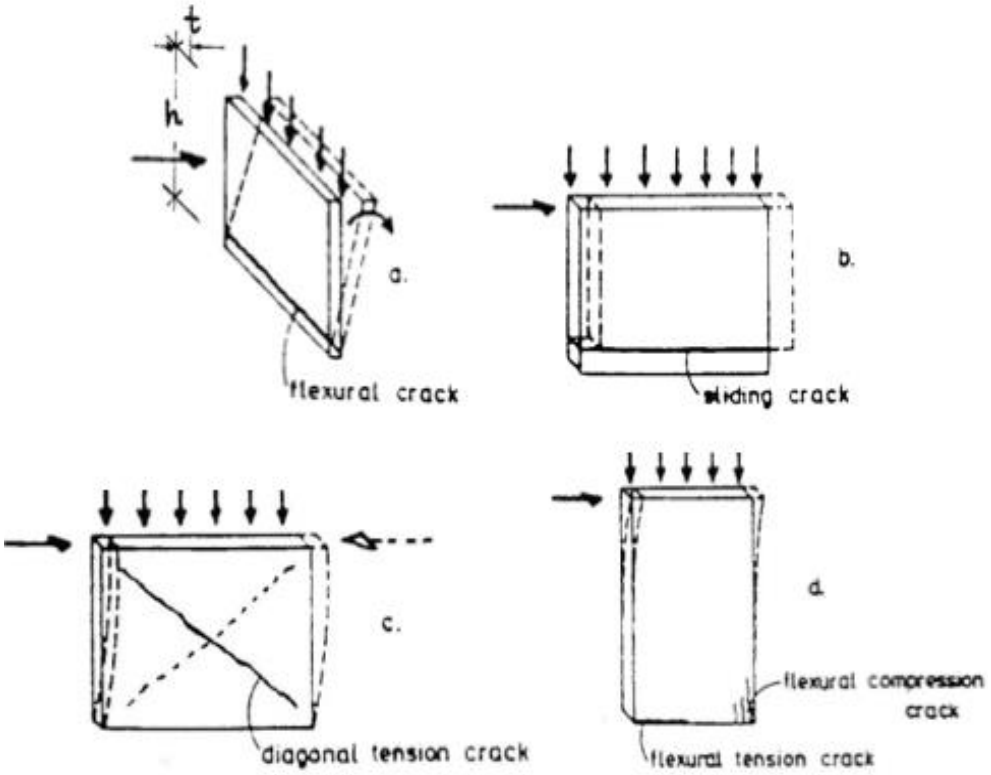

Fig. 3: Failure mechanisms of a single wall or pillar [4].

Crosswise cracking due to the main tensile stresses, either with stair-shaped, detachment-sliding of the butt and horizontal joints, or through the manifestation of cracks in the stones (Fig 3c); (iii) Bending failure due to shattering, which implies many narrow vertical cracks and transverse fracture of the compressed corner at the base, following horizontal cracking across the tensile zone (Fig. 3d).

3.2 Failure mechanisms of masonry panels under seismic loading

In the case of seismic loading, masonry panels are subjected to horizontally acting seismic forces in addition to the vertical loads [5]. Depending on the interplay between horizontal and vertical loads and between height and length of the masonry panels, various forms of failure can occur, which can basically be divided into shear, compression and tension failure.

Joint failure occurs for small load values and the stones usually remain intact, see Fig. 4. For bending failure under cyclic loading, the hysteresis loop traced is quite

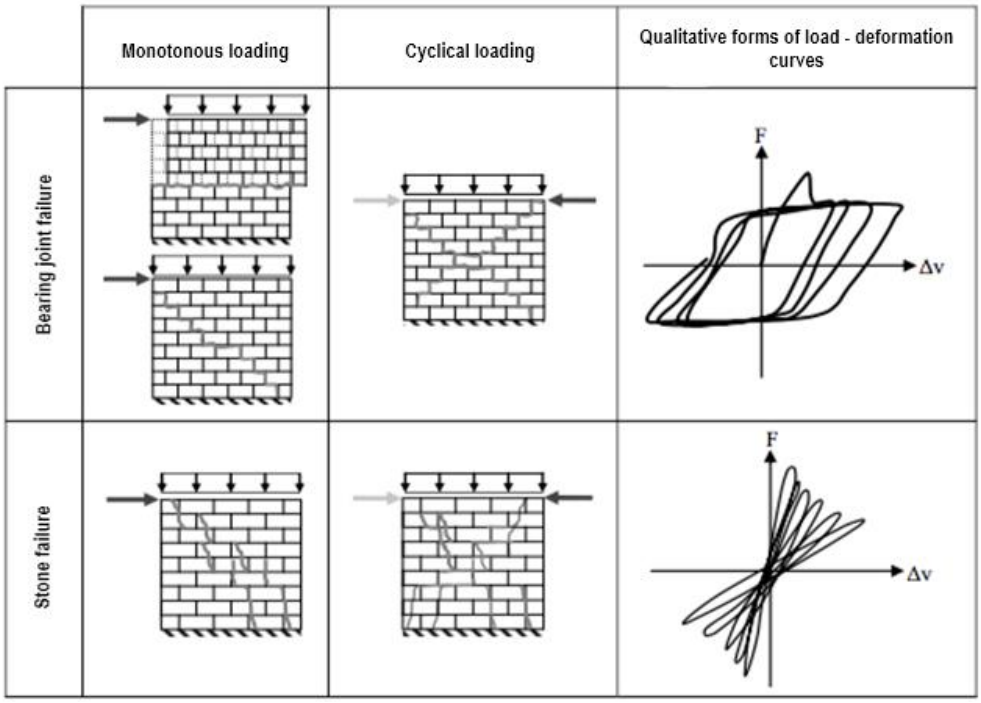

Fig. 4: Shear failure modes of masonry walls [5].

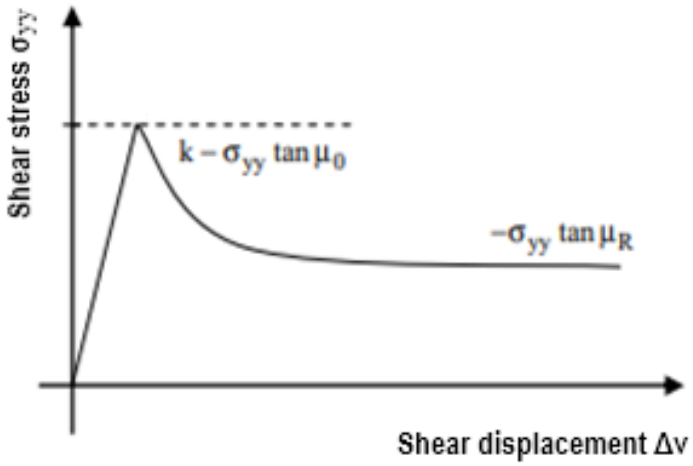

Fig. 5: Masonry bearing joint failure curve [5].

wide, signifying energy absorption. By way of contrast for shear failure the stiffness drops rapidly with little energy absorption. More specifically, shear strength depends on the angle of friction μ and on the cohesion, or rather the shear strength k (Fig. 5). The shear strength k exponentially degrades after reaching its peak value, while the friction angle μ_0 reduces to a residual value μ_R. The path of the cracks is either limited to a single bearing joint, otherwise the cracks run along the butt and bearing joints in a step-like fashion depending on the formation of the joints. The shear strength of the masonry is therefore dependent on the size of the stones, the overlap dimension (the distance between two consecutive vertical joints) and the thickness of the joints. An increase in the compression stress causes failure of adjacent stones following initial joint failure, finally resulting in a crack pattern with failure in both the joints and stones. When heavy loads induce high compressive stresses, fracture occurs exclusively through stone failure. This type of failure results from the stone rotations that occur under shear, which cause large stresses during the shearing process and results in high principle tensile stresses that lead to stone tensile failure. In essence, both joint failure and stone tensile failure are forms of shear failure.

Under alternating cyclical loading, cross cracks form (see Fig. 6), mostly due to a combination of joint with tensile stone failure. A qualitative comparison of the load-deformation curves (hysteresis curves) for these two types of failure illustrates the different modes of action under cyclic loads. When slipping at the bearing joints occurs, energy is dissipated by friction. The hysteresis curves are fully developed

Fig. 6: Cross cracks on masonry walls due to seismic loading [5].

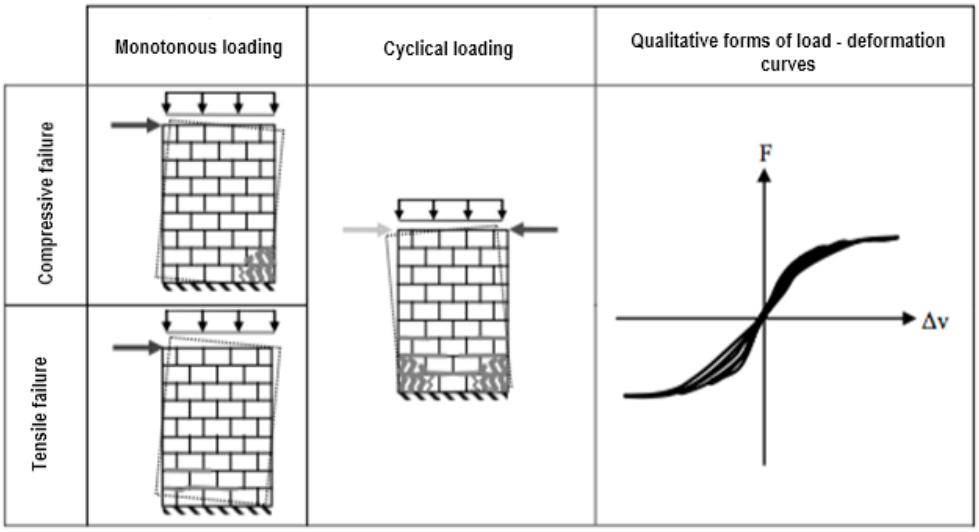

Fig. 7: Combined compressive and tensile failure due to bending in slender masonry walls [5].

and the mechanical behavior after exceeding the adhesive shear strength can be described as ductile. This behavior approximately corresponds to elastoplastic material behavior. The stone tensile failure, on the other hand, is brittle, which is manifested by less fully developed hysteresis loops. In addition, both stiffness and load bearing capacity decrease significantly after each cycle, as indicated by the flattening out of the hysteresis loops.

Next, slender masonry units are mainly stressed by bending. In this case, the governing factor for failure depends on the tensile and compressive strength of the masonry at the corner areas (see Fig. 7), while the shear load capacity plays a subordinate role here. Cyclical loads lead to tilting movements in slender walls, and there is an alternation of gaps due to changing tensile and compressive loads at the corner areas. The deformations are large in relation to the supported load and the hysteresis curves have a strongly constricted, S-shaped shape, since little energy is dissipated after initial joint rupture. At the origin, the gradient of the curves decreases only very slightly. The S-shaped shape is not so much the result of material degradation, but rather of the reduction of the suppressed cross-sectional area with increasing deformation.

It should finally be noted that total failure of a masonry unit is usually a combination of the types of failure previously described. A clear separation of the failure types described here from a mechanical point of view is usually not observed in the damage patterns of seismically damaged walls.

3.3 WALL-TO-FLOOR INTERACTION EFFECTS

The global behavior of masonry structures is influenced by interaction between individual walls in the floor plan and the floor slabs. In the case of horizontal loading, the masonry panels do not function as continuous panels with tension transmission as happens in reinforced concrete structures. In this case, the walls exhibit rotations at each floor [5]. They remain standing, and this initiates the formation of compression diagonals between the wall corners. This results in a clamping effect on the wall through the slab at each floor. This effect is stronger for short walls due to larger rotations, as compared to long walls that respond in shear (see Fig. 8). This interaction between wall and slab has a direct effect on the distribution of bending moments in the wall. In order to determine the clamping effect, factor α (see Fig. 9) is introduced, which is calculated as the quotient of the wall height h to the inflection point

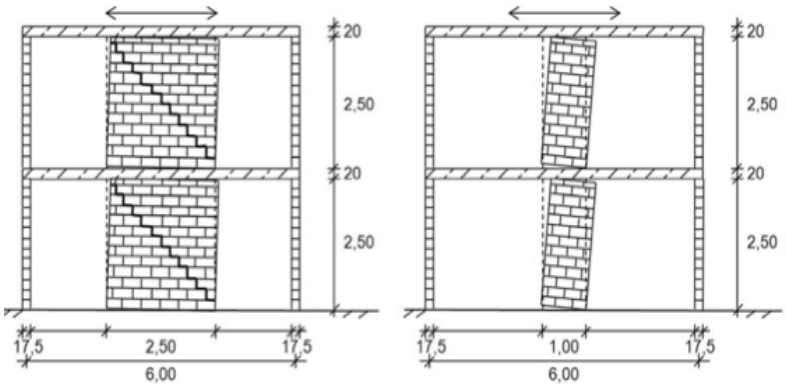

Fig. 8: Load transfer mechanism of long and short walls in masonry buildings [6].

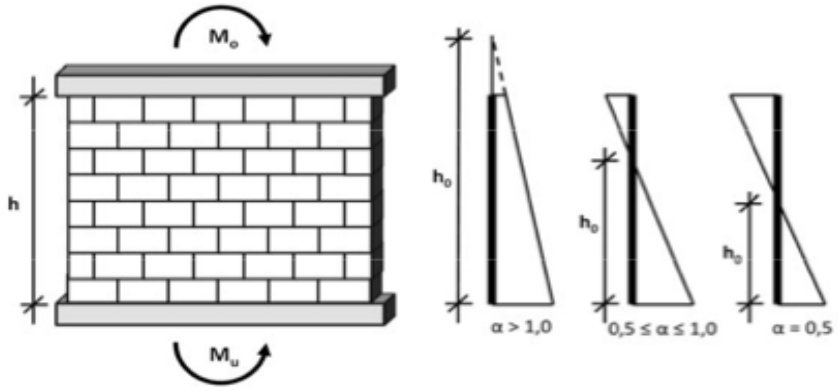

Fig. 9: Moment distribution in a single wall and corresponding clamping grade [7].

of the bending moments h_0. If the load on the wall head and foot is the same, then the degree of clamping is infinite. Theoretically, one can say that a clamping degree lies between the values $0.5 < \infty$, while negative values for the clamping degree are excluded [5]. Since the earthquake loads are cyclic, the direction in which the walls rise change. This results in a variation of the degree of clamping at the wall head and consequently, the slab is subjected to alternating bending stresses.

4 Determination of Load-Deformation Curves for Masonry

In order to determine load-deformation curves for shear walls made of unreinforced masonry, the following options are available:

(a) experimental studies;

(b) numerical simulations; and

(c) empirical formulas.

In general, it is not easy to determine these curves, as they depend on the stone-brick-mortar combination, the vertical load, the wall geometry and the self-aligning effect provided through the slabs at the wall head. There are many possible combinations and therefore experimental investigations only deal with benchmark tests, so as to help gauge numerical simulations and analytical approaches for a general description of these curves [5].

4.1 Cyclic shear wall experiments on single walls

The load-bearing and deformation behavior of masonry walls under cyclic shear loading has been investigated experimentally in various research projects to date. Of particular importance are the results of the European research projects termed DISWALL [8] and ESECMaSE [9], which have led to a better understanding of the aforementioned behavior of masonry walls. A typical arrangement for cyclic shear wall tests is shown in Fig. 10. The boundary conditions for slab clamping are simulated by means of vertical hydraulic actuators. The cyclical load history is simultaneously applied to the wall head via an articulated horizontal hydraulic actuator [10,11]. Variations in this test arrangement from other researchers will follow in Section 7. Due to many influencing parameters and high costs, it is not possible to determine nonlinear load-deformation curves by experimental investigations only. As previously mentioned, cyclic shear wall tests are benchmark tests which, together with analytical and/or numerical approaches, are used to determine the load deformation curves.

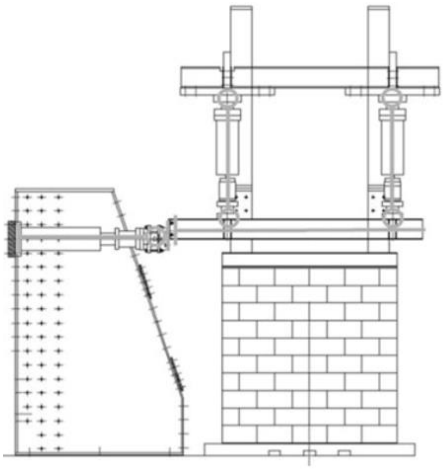

Fig. 10: Test arrangement for story high masonry wall specimens [12].

4.2 Bilinear idealization of the experimentally obtained curves

In order to idealize the test curves as bilinear, the initial stiffness, the maximum horizontal load capacity and the maximum deformation are introduced. According to [3], the plastic limit load F_y and the maximum plastic displacement $d_{\max}$ must first be determined. In the next step, the initial stiffness of the bilinear curve idealization is calculated from energy equivalence between the areas under the real and the idealized curves, from which the yield deformation d_y can be determined, see Fig. 11. This yields the deformation energy E_m below the actual load-deformation curve as a stripped area in Fig. 11. Along the same lines, [13] proposed another approach, where the maximum horizontal load capacity $V_{\max}$ and displacement $d_{\max}$ are read directly from the test curve and are used as input variables (see Fig. 12).

The guidelines of FEMA [14–17] provide formulas for calculating the maximum horizontal load bearing capacity and for the idealized curves that describe the deformability of shear walls as a function of their specific failure modes. As a result of shear loading, the bearing joint failure and the stone tensile failure are considered as failure modes. In addition, the tilting movement of the wall and the tensile and compressive failure in the corner areas of the wall base are also considered as forms of failure. Besides the individual forms of failure, combinations are also possible. More specifically, [14] introduces the following failure modes:

(a) rocking;

(b) bed joint sliding;

(c) diagonal tension; and

(d) toe crushing.

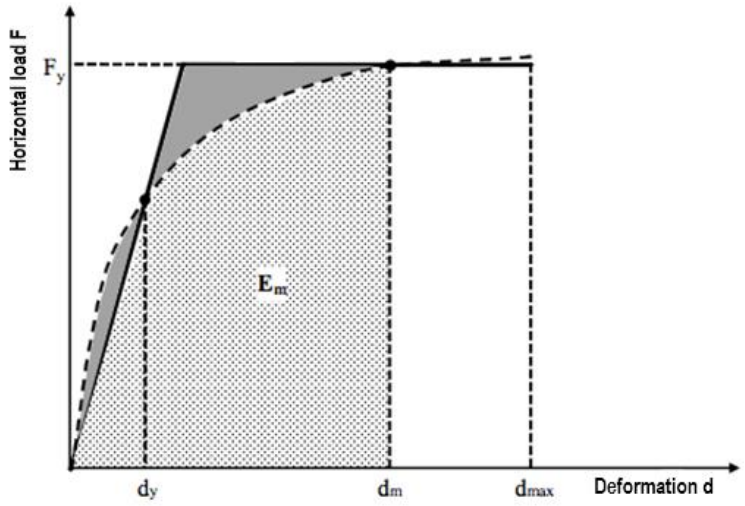

Fig. 11: Nonlinear pushover curve with its bilinear approximation [5].

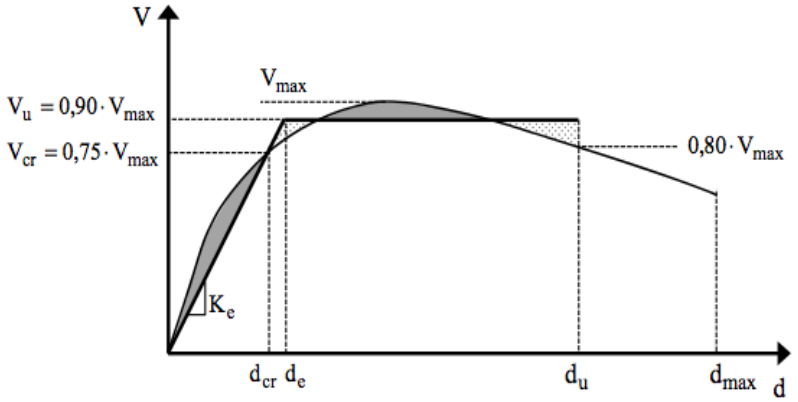

Fig. 12: Bilinear idealization according to [13].

4.3 Determination of deformation capabilities for each failure mode by FEMA

For each failure mode in the FEMA guidelines, there is an associated deformability. In principle, there are ductile, semi-ductile and brittle forms of failure. When unreinforced masonry is considered, the failure modes labelled “rocking” and “bed joint sliding” are ductile failure modes with a pronounced amount of deformation. The corresponding idealized load-deformation curve is shown in Fig. 13. Values for $V_{\max}$, c, d and e (the maximum shear value and distance markers depicted in Fig. 13)

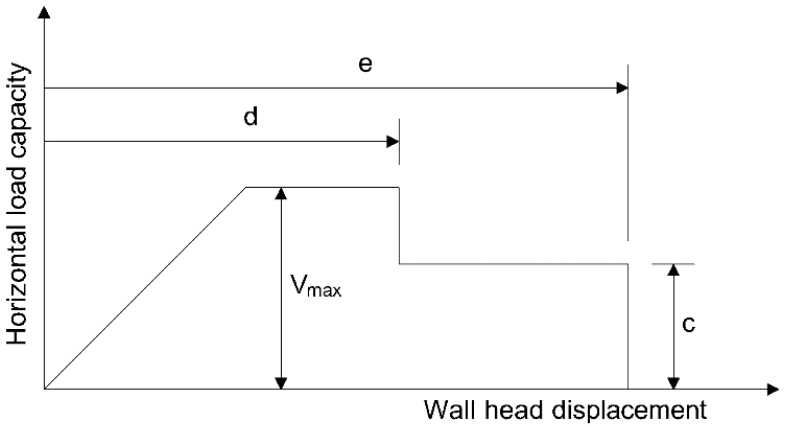

Fig. 13: Idealized loaddeformation relation according to [17].

are calculated according to Table 1, and since they were derived directly from shear wall tests, they are augmented by safety factors. For a behavior oriented seismic design, the deformation capabilities are limited by the guidelines in [17] under the requirements for "life safety" (LP) and "collapse prevention" (CP).

Table 1: Limit values for the deformation capacity according to FEMA guidelines

Failure mode	$V_{\max}$ [kN]	c [kN]	d [m]	e [m]	LS [m]	CP [m]
Bed joint sliding	V_{bjs1}	V_{bjs2}	$0.004h_w$	$0.008h_w$	$0.003h_w$	$0.004h_w$
Rocking	V_r	$0.6V_r$	$0.004h_w^2/l$	$0.008h_w^2/l$	$0.003h_w^2/l$	$0.004h_w^2/l$

Rocking occurs when the bed joints at the top and the bottom of the wall tear and the wall performs a tilting motion like a rigid body. The maximal horizontal load-bearing capacity V_r is calculated with the assumption that one- tenth of the wall length is the length of the compressive zone.

$$V_r = 0.9\alpha_{\text{FEMA}} N_{Ed}(1/h_w)\,. \tag{1}$$

In the above, N_{Ed} is the centric compressive force, l is the wall length and h_w is the wall height. The factor α_{FEMA} considers the degree of restraint on the wall head ($\alpha_{\text{FEMA}} = 1$: restrained; $\alpha_{\text{FEMA}} = 0.5$: articulated).

Bed joint sliding occurs when the absorbable horizontal load-bearing capacity of the bed joints is exceeded. The horizontal load bearing capacity V_{bjs1} results from the product of the shear strength f_{vk} times the mortared area A. The shear strength

f_{vk} is a function of the adhesive shear strength f_{vk0} and of the compressive stress perpendicular to the bed joint σ_{Dd}, which in turn is dependent on static friction at the surface that manifests a coefficient of static friction μ_{sf}. Thus we have that

$$V_{bjs1} = f_{vk}A = (f_{vk0} + \mu_{sf}\sigma_{Dd})A\,. \tag{2}$$

After exceeding V_{bjs1}, sliding occurs in the bed joints and the remaining horizontal load-bearing capacity V_{bjs2} is calculated using the coefficient of sliding friction μ_{df} as follows:

$$V_{bjs2} = \mu_{df}\sigma_{Dd}A\,. \tag{3}$$

4.4 Analytical approaches in EN 1998-3

Code EN 1998–3 [18], Annex C, defines the capacity models for individual masonry walls as an aid in examining existing structures. A distinction is made between walls under bending, under longitudinal loading and under shear loading. It should be noted that the approaches in [18] are based on much older tests with normal mortars and mortar-based butt joints, so that a direct transfer to today's modern masonry construction is questionable [5]

4.5 Determination of deformation capabilities for each failure mode by Eurocode

In [18], certain limits for the deformation are specified at different failure modes as a function of floor displacement. In comparison to the approach of the [17] guidelines, the post-crushing area is completely disregarded. The approach in this case is limited to an elastoplastic load-deformation curve by specifying the limit displacement, which is marked as d (see Fig. 13). The limit displacements for each failure mode are also shown in Table 1.

4.6 Analytical approach based on experimental data from EU research projects

Reference [7] developed an approximate method for the bilinear idealization of the load-deformation curves of masonry shear walls. These findings were based on an evaluation of the test results from the European research project ESECMaSE [9]. This approach followed the German regulations DIN EN 1998–3 [19], but the load-bearing and deformation capabilities of masonry were modified. It has been shown that the approach according to [19] provides high values for the load-bearing and deformation capabilities as compared to the results from project ESECMaSE [9]. Therefore, it cannot be applied directly to modern masonry, as already mentioned

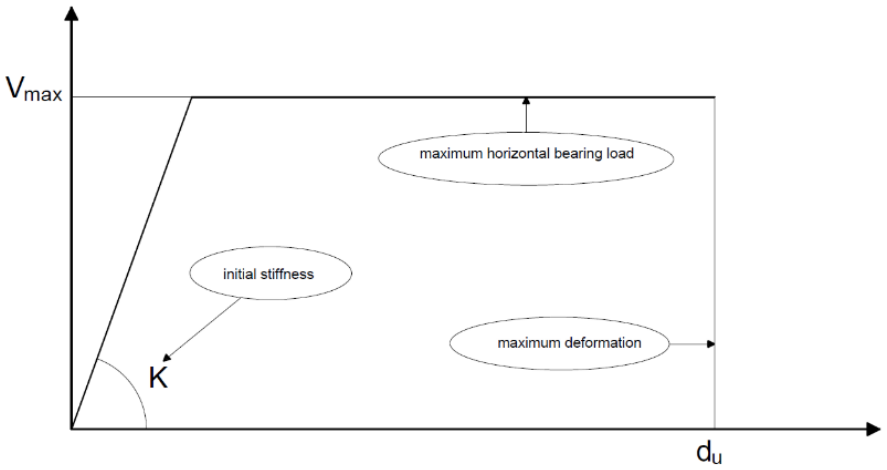

Fig. 14: Bilinear idealization of the load-deformation curves [20].

before. The approximate method takes into account the fracture conditions, shear failure due to friction failure (SS), shear failure due to stone tension failure (SZ) and the bending and longitudinal force (BL). The load-bearing and deformation capabilities can be determined separately for each fracture condition. The advantage of this approach is that only the bonding shear strength f_{vk0} and the masonry compressive strength f_k are required as input values for the material properties, which can be easily determined using standard testing methods. Figure 14 shows the bilinear idealization of the load-deformation curve for the approximate method, which is defined by the initial stiffness, the maximum horizontal load capacity $V_{\max}$ and the maximum deformation d_u. The load-bearing and deformation capacities were calculated according to Table 1, while the maximum horizontal load-bearing capacity is the smallest of the three fracture conditions. The maximum final deformation is the one corresponding to the controlling fracture condition.

5 Regulations Governing the Design of Masonry Walls

The regulations governing masonry design and construction can be divided in those that describe experimental setups, according to which the mechanical properties of both masonry and mortar are calculated, and in those that are used in order to design masonry walls. It should be noted that not all regulations explicitly follow European standards.

5.1 Regulations on the calculation of mechanical properties

ASTM E519-10 [21]: Standard test method for diagonal tension (shear) in masonry assemblages.

ASTM E447 [22]: Standard test methods for compressive strength of masonry prisms.

ASTM E2126-02a [23]: Standard test methods for cyclic (reversed) load test for shear resistance of framed walls in buildings.

EN 1015-11 [24]: Methods for testing mortar in masonry. Determination of flexural and compressive strength of hardened mortar.

EN 1052-1 [25]: Methods for testing masonry. Determination of compressive strength.

EN 1052-2 [26]: Methods for testing masonry. Determination of flexural strength.

EN 1052-3 [27]: Methods for testing masonry. Determination of initial shear strength.

DIN 18946 [28]: Earth masonry mortar. Terms and definitions, requirements, test methods.

RILEM TC 76-LUM [29]: General recommendations for testing load bearing masonry.

5.2 Regulations on the design of masonry walls

Eurocode 6, Part 1-1 [2]: General rules for reinforced and unreinforced masonry structures.

Eurocode 8, Part 3 [18]: Assessment and retrofitting of buildings.

NTC 08 [30]: Italian code for structural design.

Ordinanza OPCM 3274 [31]: Italian seismic code.

IMIT (2009): Italian building code commentary.

Table 2: Reference values for the mechanical parameters of existing masonry [32]

Masonry type	Compress strength f_m (MPa) min/max	Shear strength τ_0 (MPa) min/max	Elastic modulus E (MPa) min/max	Shear modulus G (MPa) min/max	Weight density W (kN/m^3)
Irregular stone	1.0/1.8	0.020/0.032	690/1050	230/350	19
Uncut stone	2.0/3.0	0.035/0.051	1020/1440	340/480	20
Cut stone with good bond	2.6/3.8	0.056/0.074	1500/1980	500/660	21
Soft stone	1.4/2.4	0.028/0.042	900/1260	300/420	16
Dressed stone (ashlar)	6.0/8.0	0.090/0.120	2400/3200	780/940	22
Solid brick (lime mortar)	2.4/4.0	0.060/0.090	1200/1800	400/600	18

Table 3: Multiplication factors of existing masonry properties provided by [32]

Good quality mortar	1.5	Thin bed joints	1.5
Transverse connections (headers)	1.3	Weak mortar and/or wide inner core	0.7
Grout injections	1.5	Ferrocement	1.5

Tables 2 and 3 contain numerical values for the mechanical properties of various types of existing masonry walls, based on the commentary of the Italian building code IMIT [32]. Table 1 provides values of a multiplication factor for other wall typologies that are not contained on the Table 2. The combined information from these tables allow calculations for 36 typologies of idealized masonry walls.

6 Numerical Methods for Masonry Walls

In what follows, we will discuss the basic philosophy behind modelling masonry walls through the use of general-purpose software.

6.1 Simplified numerical approaches using macro-elements

The FME (frame by macro-elements) method results from a consideration of the actual damage to buildings exposed to an earthquake and accounts for the various failure mechanisms that are possible. In the case of a finite element method (FEM) calculation, 'small' elements are defined which, depending on their size, describe the masonry structure in a satisfactory way. In contrast, macro-elements have large dimensions that combine areas of the structure with the same load-bearing behavior.

A masonry wall can comprise different components, namely pier, spandrel beam and rigid elements. Figure 15(a) shows such an arrangement. More specifically, pier elements are located at the side of the openings and transfer both vertical and horizontal loads to the floor slabs. They are in essence the stiffening parts of a masonry wall. Spandrel beam elements are located above and below the wall openings, take on vertical and horizontal loads and transfer them to the pillar elements. Everything else that remains on a masonry wall and does not border an opening, can be regarded as a rigid element. The connection of pillar elements, bar elements and fixed nodes results in an equivalent frame arrangement, see Fig. 15(b) for an example. This implies that beam finite elements with properties derived from the previously mentioned structural elements can be used, which considerably simplifies subsequent calculations. Implementation of the FME method was done by developers of the general-purpose computer program 3MURI [33], in which the simplified macro-element model used is characterized by bilinear inelastic behavior from a standard pushover analysis. The meshing of the model is done automatically by the program and changed to manual if so desired.

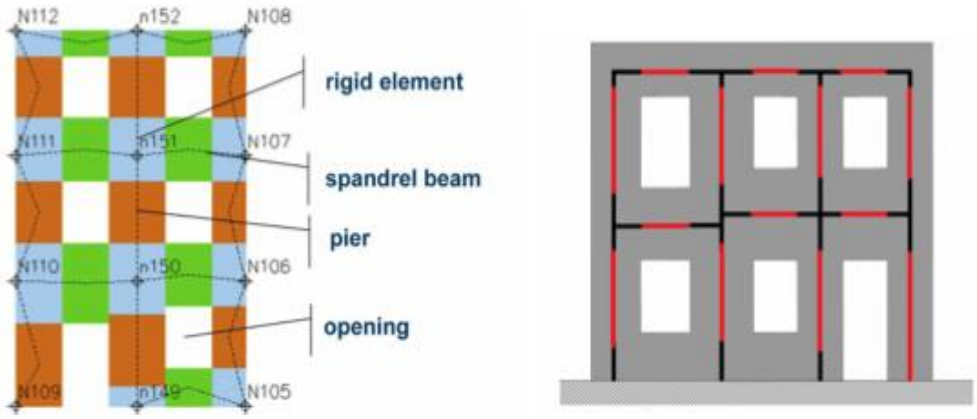

(a) (b)

Fig. 15: (a) FEM meshing of a typical wall and (b) equivalent frame model [33].

6.2 Advanced numerical approaches using macro-modelling

Macro-modelling is a FEM variant known as the continuum mechanics FEM. According to this method, no distinction is made between the joints and the stone/brick units. Furthermore, damage is described as a scattered property through-out the volume of the structure, and hence the designation of a 'smeared crack' approach. An-

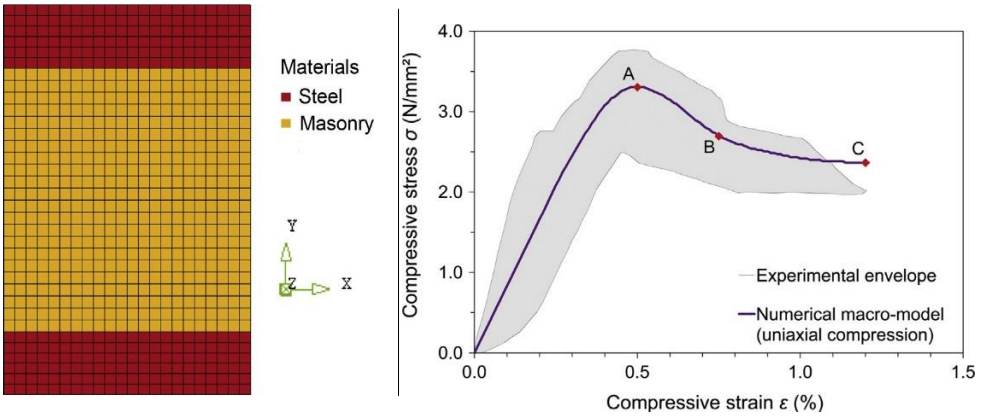

(a) (b)

Fig. 16: (a) FEM mesh and composition for the macro-modelling of a small wall specimen (wallette) tested under uniaxial compression and (b) comparison between experimental and numerical results [36].

other assumption is that masonry is considered as a homogenous and continuous material. Given the small computation cost of this method, accuracy of the results is low. For this reason, it is being used only for the sake of efficiency, when high accuracy in the results is not an issue. The method also finds application in rubble stone masonry, where crack formation cannot be forecast. By way of contrast, the method is unstable in comparison to the distinct crack approach, when complete material degradation must be recovered. A commercial software that utilizes macro-modelling is DIANA FEA [34], formerly known as TNO DIANA [35]. Figures 16 and 17 depict the modelling of experimental setups using DIANA FEA [34] and show a comparison between numerical and experimental results [36]. In Fig. 16a a wall specimen (wallette) is tested under uniaxial compression. The specimen is constrained between two rigid beams (red colored mesh). The same finite element type is adopted for both the wallette and the steel elements (the 8-node quadrilateral element). In Fig. 16b it is obvious that the macro-model and the experimental test results are in agreement in terms of uniaxial stress-strain behavior. In Fig. 17a a wallette is tested under diagonal compression and is modelled similarly to the previously mentioned model. The specimen is placed between two steel shoes (red colored mesh) which are used to apply the diagonal load. For the steel elements, 6-node triangular elements were used, whereas for the wallette, 8-node quadrilateral elements were used. As depicted in Fig. 17b, a good approximation between experimental and numerical results is obtained.

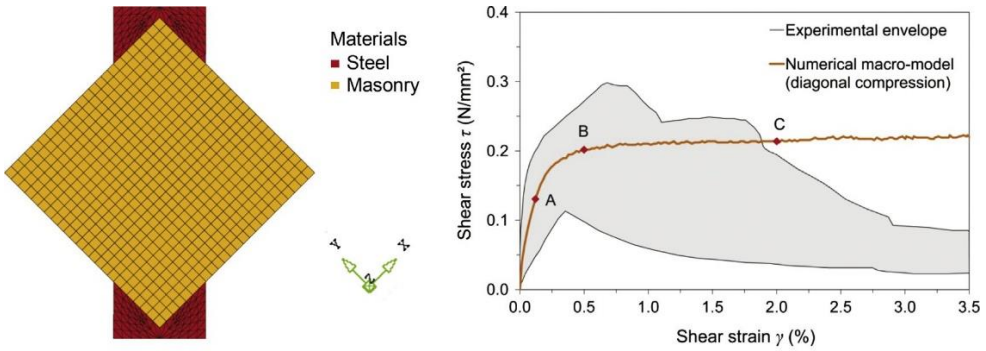

(a) (b)

Fig. 17: (a) Mesh and materials for macro-model of a small wall specimen (wallette) tested under diagonal compression and (b) comparison between experimental and numerical results obtained with the Mohr-Coulomb criterion [36].

6.3 Advanced numerical approaches using micro-modelling

Micro-modelling, as well as macro-modelling are FEM-based approaches. In the so called detailed micro-models, the individual units and the mortar of the joints is modeled with continuous finite elements, whereas the unit-mortar interface is modeled with discontinuous finite elements, which describe potential fracture and identify sliding locations. The latter method accounts for potential fractures throughout the units and is reliable from a convergence point of view. When compared to the use of 'smeared crack' models for the units, it is effective in recovering a wall response characterized by over-strength. Specifically, micro-modelling produces reliable and accurate results but has a high computational cost. This issue can be partially overcome with the application of simplified methods and the assumption that masonry is considered as a set of elastic blocks bonded by potential fracture/slip lines at the joints. The basic disadvantage of micro modelling is because of the high computational cost it is suitable only for small elements or for looking at wall details. A commercial software that is based on micro-modelling is again DIANA FEA [34]. Figures 18 and 19 depict modelling of some experimental setups with DIANA FEA [34] and show a comparison between the numerical and the experimental results [36]. In Fig. 18a a wall specimen (wallette) is tested under uniaxial compression and the actual arrangement of earth blocks and mortar joints is taken into account. The specimen is constrained between two rigid beams (dark gray mesh). The same finite element type is adopted for both the wallette and the steel elements (the 8-node quadrilateral ele-

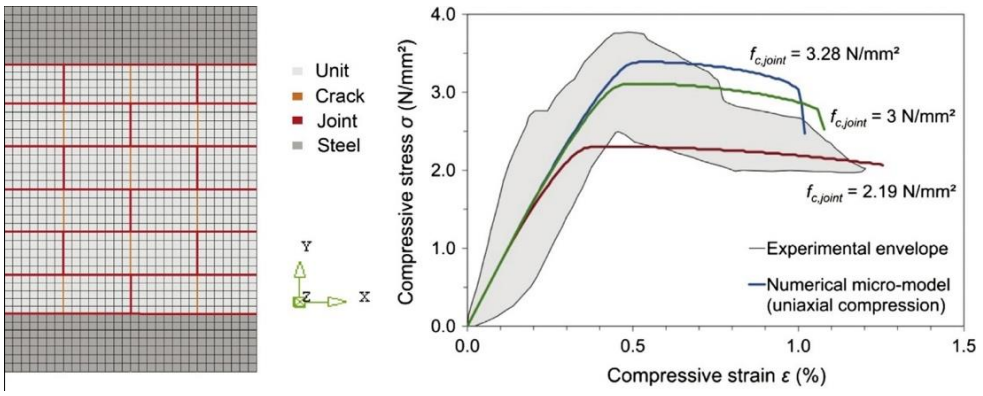

(a) (b)

Fig. 18: (a) Mesh and materials for micro-model of a small wall specimen (wallette) tested under uniaxial compression and (b) comparison between experimental and numerical results [36].

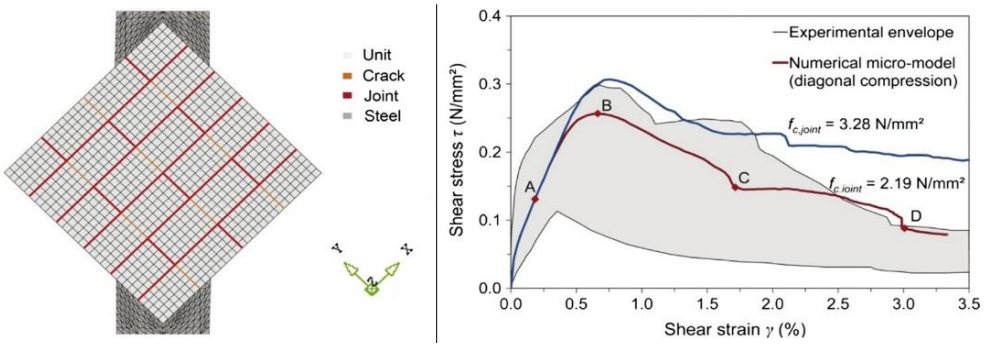

(a) (b)

Fig. 19: (a) Mesh and materials for micro-model of a wall specimen (wallette) tested under diagonal compression and (b) comparison between experimental and numerical results [36].

ment). The interfaces (joints and block cracks) were modelled using line elements. Figure 18b depicts the micro-model and the experimental test results. The three colored curves correspond to different values of the interface compressive strength that were taken into account. In Fig. 19a, a wallette is again tested under diagonal compression and is modelled similarly to the previously mentioned model. The specimen is placed between two steel shoes (dark gray mesh) which are used to apply the diagonal load. For the steel elements, 6-node triangular elements were used, whereas for the wallette, 8-node quadrilateral elements were used. Figure 19b compares the micro-model and the experimental test results. The two-colored curves correspond to different values of the interface compressive strength that were taken into account. Only the lower of the two interface values led to a curve that was in good agreement with the experimental results, while the other one only approximated them.

6.4 The discrete element method

The Discrete Element Method (DEM) is a method initially developed for rock mechanics. Due to its numerical robustness and its ability to simulate the interaction between the elements (or blocks of elements), this method is a viable alternative for calculations involving masonry structures. According to this method, each block simulates a stone modeled by a finite difference mesh. It utilizes the Voronoi [37] algorithm for element/block generation. The main difference between DEM and FEM is that in the former case, the complete load-displacement curve is reproduced, although great attention to convergence is required, whereas with the latter, only the maximum load applied can be computed, but without much attention paid to conver-

gence between the solution steps. The notation 'discrete' derives from the fact that finite displacements and rotations between bodies are allowed, including complete detachment, plus the ability of identifying new contacts automatically, as the calculations propagate. The DEM is characterized by the simulation of the material as a configuration of discrete blocks that interact along their borders. Finally, different formulations of this method are:

(a) the distinct element method;

(b) the discrete finite elements;

(c) the discontinuous deformation analysis.

A commercial software that utilizes the DEM is UDEC [38], released by the Itasca Group.

7 Experimental Testing of Masonry Walls

We list here some of the most important tests that have been performed on masonry walls in the recent past. Specifically, we have:

(a) The team in Ref. [39] performed a series of tests in order to calculate the diagonal tension strength of rubble stone masonry panels. In order to characterize the shear strength of those panels, they performed diagonal compression tests according to [21]. The dimensions of the four specimens used were $120 \times 120 \times 70$ cm. Those experiments were done with the aim to obtain the shear strength of the panels, their shear modulus and their diagonal tensile strength. They also tested the flexural strength of the mortar according to [24], which is the mortar tensile strength obtained by bending tests and used nine prismatic specimens with the dimensions $160 \times 40 \times 40$ mm.

(b) The team in Ref. [40] performed experiments in order to examine stone masonry in shear and compression. Shear tests of masonry joints are normally executed according to [27] (the triplet test), whereas the compressive response is examined according to [25]. Due to technical reasons and for simplicity, the team performed the tests with some variations. For instance, the shear strength of the joints was examined with the direct shear test on couplet specimens, because it is easier to test one joint instead of two simultaneously. The tests were performed under monotonic as well as under cyclic loading conditions. The compressive strength on the other hand was tested on prismatic specimens due to the very high strength of granite stones and the maximum capacity of the actuators that were available for testing.

(c) The team in Ref. 36] conducted experimental tests on earth block masonry. Each earth block had dimensions of $240 \times 115 \times 71.5$ mm and the preparation of the

mortar was made according to [28]. The shear test was executed according to [27], procedure A, and the pre-compression loads applied were in the range specified by [28]. The compression test was executed on earth block wall specimens (wallettes) of size $500 \times 500 \times 115$ mm which were built according to [25]. These blocks were connected by 20 mm joints, which is wider than what is recommended by the standards, because wider joints are often observed in historic earth block masonry. The diagonal compression test was performed in accordance to [21]. A photogrammetric camera system (ARAMIS) measured the two-dimensional deformation during the test on a sample surface of the dimensions 25×35 cm. It is also worth to mention that before the beginning of the test the samples were plastered with a thin white gypsum render and sprayed with a marker.

(d) The team in Ref. [41] performed a new series of tests in order to examine the seismic response of rubble stone masonry panels by means of static cyclic tests. They first examined the mortar flexural strength, which is the tensile strength of the mortar obtained from bending tests. The tests were performed on nine prismatic specimens with dimensions $160 \times 40 \times 40$ mm according to [24]. Following the flexural strength tests, they also performed compressions tests on the half-prisms used before. Finally, they performed static cyclic shear tests on four $120 \times 120 \times 40$ cm specimens. They used two types of mortar, namely hydraulic lime mortar corresponding to newer buildings and air lime mortar corresponding to older buildings. The specimens were tested twelve months after construction to ensure proper mortar hardness and the stones used were roughly cut limestone. Static cyclic horizontal loads were applied on top combined with a pre-compression level, in accordance with [23]. Transducers were placed on the sides of the specimens in order to leave the front and back surfaces free to better observe and register the cracks during the tests. It is also worth to mention that each load cycle was repeated three times, something that is common for such type of testing.

(e) The team in Ref. [42] performed a series of tests in order to calibrate and apply a continuum damage model to the simulation of stone masonry structures. The tests were performed on $160 \times 160 \times 60$ cm walls made from granite stones. Some of the stones were polished along the transverse direction of the walls in order to connect the leaves and improve global behavior. The walls were built on a $1.6 \times 2.6 \times 0.6$ m concrete block that simulated the foundation with a fixing depth of 0.35 m. These walls were tested with a constant vertical load and controlled horizontal in-plane cyclic displacements. The foundation block was fixed on the laboratory reaction floor, in order to avoid any displacement of the block during the test. It has been shown from the tests that even identical wall setups can behave differently due to local effects.

7.1 Discussion of the experimental results

Conclusions drawn from the aforementioned experimental testing are as follows:

(a) Based on the test by [40], it is important to mention that the shear strength of the mortar-stone interface, as well as the compressive strength of masonry stone are basic mechanical properties necessary for both numerical modeling and for design of stone walls. It was observed that what governs the shear behavior of masonry joints, is the elastic-perfectly plastic, shear stress-displacement diagram. This was found to characterize the monotonic and the cyclic envelope of dry masonry joints, whereas post-peak strength degradation and a consequent stabilization characterizes the monotonic behavior of mortar joints. The moisture content on the joints, from dry to saturated, seems to have a negligible effect on the friction coefficient. Furthermore, dilatancy did not influence the shear behavior of dry masonry joints, whereas dilatant behavior was observed in mortared joints. Next, the shear strength property of masonry joints enables the assessment of the in-plane lateral strength of masonry walls under in-plane loading. What was observed to control the compressive behavior of masonry is the surface condition, be it smooth or rough. This influences the composite behavior of masonry under compression, mostly with respect to the compressive strength, the modulus of elasticity and the deformation at peak stress. The material of the bed joints, either lime mortar or clay material, considerably influences the failure mode and the compressive strength of stone masonry. The different bed joint materials lead to clear and distinct pre-peak regimes in the stress-strain diagrams, resulting in very a different modulus of elasticity, compressive strength and permanent deformations after a number of loading-reloading cycles. The materials of the bed joints play a central role on the deformation behavior of stone masonry under compressive loading. Finally, as with the shear strength properties of masonry joints, also the compressive strength of stone masonry represents an important parameter for the assessment of the in-plane and out-of-plane strength of masonry walls.

(b) Based on the tests by [36] previously described, the following conclusions regarding the shear strength, the uniaxial compressive strength and the failure under shear loading can be drawn:

(i) The two different pre-load sets used during the drying phase had no significant impact on the shear strength of the walls;

(ii) the brittle behavior of earth block masonry under uniaxial compressive load was confirmed; and

(iii) failure under shear load occurs by sliding of the earth blocks along the mortar joints after initial cracking in mortar joints and earth blocks.

(c) Based on the tests by [39,41], the following conclusions about the stone layout, the mortar type, the energy dissipation and the failure mode can be drawn. First, the layout of the stone layout greatly influences the overall behavior of the specimens, as two of the specimens which were based on hydraulic mortar presented different behavior. Second, the mortar type has a huge influence on the results. Specimens that were built with air lime mortar showed much lower strength than the specimens built with hydraulic lime mortar. Finally, specimens that were built with hydraulic lime mortar dissipate much more energy than specimens built with air lime mortar. In all specimens tested, the stiffness and ductility of the stone walls clearly depends of the failure mode.

(d) Although the tests by [42] were conducted in order to calibrate a computational model, the following interesting conclusion regarding the energy dissipation can be made. Specifically, although the specimens tested were identical, there was a difference of 27%. In the results. This can be mainly due to local phenomena and other unstable parameters.

8 Concluding Remarks

Based on the above state-of-practice exposition, the following conclusions regarding the basic mechanical behavior of stone masonry can be drawn:

(a) The compressive strength is the most basic mechanical property of masonry construction, although it is not directly related to the seismic behavior of buildings. It is well known that masonry does not fail in compression under gravity loads. However, compression induced to a building due to seismic actions may be significantly increased in its vertical elements.

(b) To date, there is no general mechanical model that accurately describes the behavior of masonry in compression, because such a model should be able to describe the mechanical properties of various types of historic masonries [43]. It is worth mentioning that even for modern masonry construction, [2] proposes empirical formulae that are valid for construction techniques that follow specific rules. In reality, historic masonries fulfill almost none of the requirements imposed by [2], and this is the main reason why empirical formulae are proposed in the literature.

(c) Furthermore, it is worth mentioning that the deformation properties exhibited by historic masonries are quite scattered as well. Similarly, a large scatter is observed in the modulus of elasticity [43]. Failure under compression of historic masonry, with loose connection between the interconnected parallel wall layers (leaves), occurs in most cases with vertical cracks on the masonry faces, as well as within their thickness. Although these two types of cracks open at the same vertical load values, the transverse ones grow faster and failure occurs due to simultaneous compression and out-of- plane flexure of the leaves.

(d) The behavior of masonry under shear loads is the most significant for the seismic response of masonry structures. The most common dimensions of wall specimens tested under shear conditions varies between the 1: 2 and 2: 1 height to length ratios. The most common failure mode involves the formation of diagonal or bi-diagonal cracks. Flexural failure or mixed shear-flexural failure can also be observed for high aspect ratio values. In addition, rocking was also observed in some cases.

(e) To conclude, it is important to mention that the most critical parameters that influence the shear strength of masonry construction are the mechanical parameters of its individual components, as well as the bond between stones, bricks and mortar.

REFERENCES

[1] C.C. SPYRAKOS (2019) "Masonry Construction: Evaluation and Retrofit for Seismic Loads" (in Greek). Ergonos Publishing House, Athens.

[2] EN 1996-1-1 (2005) "Eurocode 6: Design of Masonry Structures – Part 1-1: General Rules for Reinforced and Unreinforced Masonry Structures". European Committee for Standardization (CEN), Brussels, Belgium.

[3] EN 1998-1 (2004) "Eurocode 8: Design of Structures for Earthquake Resistance – Part 1: General rules, seismic actions and rules for buildings". European Committee for Standardization (CEN), Brussels, Belgium.

[4] G. PAPADOPOULOS (2014) "Validierung von Bemmesungskinzepten textilverstärkten Mauerwerks". Masterarbeit, Lehrstuhl für Massivbau, Karlsruher Institut für Technologie, Karlsruhe, Germany.

[5] K. MESKOURIS, K.G. HINZEN, C. BUTENWEG, M. MISTLER (2011) "Bauwerke und Erdbeben-Grundlagen, Anwendung, Beispiele". Vieweg+Teubner Verlag, Wiesbaden, Germany.

[6] C. BUTENWEG, C. GELLERT, U. MEYER (2010) "Erdbebenbemessung bei Mauerwerksbauten, Mauerwerk Kalender 2010". Verlag Ernst & Sohn, Berlin.

[7] C. GELLERT (2010) "Nichtlinearer Nachweis von unbewehrten Mauerwerksbauten unter Erdbebeneinwirkung". Dissertation, Lehrstuhl für Baustatik und Baudynamik, RWTH Aachen.

[8] DISWALL (2010) "Developing Innovative Systems for Reinforced Masonry Walls". University of Padova, Italy, http://diswall.dic.unipd.it

[9] ESECMASE (2010) "Enhanced Safety and Efficient Construction of Masonry Structures in Europe". DGM, Berlin, Germany, http://www.esecmase.org.

[10] E. FEHLING, J. STÜRZ (2006) Seismic resistance of different types of vertically perforated clay bricks. In: *Proceedings of the First European Conference on Earthquake Engineering and Seismology*, Geneva, Switzerland.

[11] E. FEHLING, J. STÜRZ (2006) Behaviour of masonry walls made from different types of clay bricks under static-cyclic loading. In: *Proceedings of the 7th International Masonry Conference*, London, UK.

[12] E. FEHLING, D. SCHERMER, J. STÜRZ (2007) Test method for masonry walls subjected to in-plane loading. In: *Proceedings of the 2nd International Conference on Advances in Experimental Structural Engineering*, Shanghai, China.

[13] M. TOMAZEVIC (2006) "Earthquake-Resistant Design of Masonry Buildings, Series on Innovation in Structures and Construction", Vol. 1. Imperial College Press, London, UK.

[14] FEMA 306 (1998) "Evaluation of Earthquake Damaged Concrete and Masonry Wall Buildings – Basic Procedures Manual". Federal Emergency Management Agency, Publication No. 306, Washington D.C., USA.

[15] FEMA 307 (1998) "Evaluation of Earthquake Damaged Concrete and Masonry Wall Buildings – Technical Resources". Federal Emergency Management Agency, Publication No. 307, Washington D.C., USA.

[16] FEMA 308 (1998) "Repair of Earthquake Damaged Concrete and Masonry Wall Buildings". Federal Emergency Management Agency, Publication No. 308, Washington D.C., USA.

[17] FEMA 356 (2000) "Pre-standard and Commentary for the Seismic Rehabilitation of Buildings". American Society of Civil Engineers (ASCE), Reston, VA., USA.

[18] EN 1998-3 (2005) "Eurocode 8: Design of Structures for Earthquake Resistance – Part 3: Assessment and retrofitting of buildings". European Committee for Standardization (CEN), Brussels, Belgium.

[19] DIN EN 1998-3 (2010) "Eurocode 8: Design of Structures for Earthquake Resistance – Part 3: Assessment and retrofitting of buildings". German Version EN 1998-3:2005+AC:2010. Deutsches Institut für Normung (DIN), Berlin, Germany.

[20] P. SCHLEMMER (2008) Ansatz zur Parametrisierung von Last-Verformungskurven für Mauerwerksscheiben. Diplomarbeit, Lehrstuhl fr Baustatik und Baudynamik, RWTH Aachen.

[21] ASTM E 519-10 (2010) "Standard test method for diagonal tension (shear) in masonry assemblages". American Society for Testing and Materials, West Conshohocken, PA, USA.

[22] ASTM E 447 (1992) "Standard test methods for compressive strength of masonry prisms". American Society for Testing and Materials, West Conshohocken, PA, USA.

[23] ASTM E 2126-02A (2002) "Standard test methods for cyclic (reversed) load test for shear resistance of walls for buildings" American Society for Testing and Materials, West Conshohocken, PA, USA.

[24] EN 1015-11 (1999) "Methods of test for mortar for masonry - Part 11: determination of flexural and compressive strength of hardened mortar". European Committee for Standardization (CEN), Brussels, Belgium.

[25] EN 1052-1 (1999) "Methods of test for masonry: Part 1 – Determination of compressive strength". European Committee for Standardization (CEN), Brussels, Belgium.

[26] EN 1052-2 (1999) "Methods of test for masonry: Part 2 – Determination of flexural strength". European Committee for Standardization (CEN), Brussels, Belgium.

[27] EN 1052-3 (2002) Methods of test for masonry: Part 3 – Determination of initial shear strength". European Committee for Standardization (CEN), Brussels, Belgium.

[28] DIN 18946 (2013). "Earth masonry mortar – Terms and definitions, requirements, test methods". Deutsches Institut für Normung (DIN), Berlin, Germany.

[29] RILEM TC 76-LUM (1994) Diagonal tensile strength tests of small wall specimens. In: *RILEM, Recommendations for the Testing and Use of Constructions Materials*, pp. 488-9; E. & F.N. Spon, London, UK.

[30] NTC08 (2008) "Nuove Norme Tecniche per le Costruzioni". Italian Ministry of Infrastructures and Transportation, G.U. n.29 – S.O. n.30, Rome, Italy.

[31] ORDINANZA OPCM 3274 (2003) modified according to OPM 3431 (2005) "Allegato 2, Norme tecniche per il progetto, la valutazione e l'adeguamento sismico degli edifici". Consiglio dei Ministri, Rome, Italy.

[32] IMIT (2009) "No. 617: Istruzioni per l'applicazione delle Nuove Norme Tecniche per le Costruzioni di cui al decreto ministeriale". Italian Ministry of Infrastructures and Transportation, Rome, Italy.

[33] 3MURI (2012) "General Description Manual", Version 4'. S.T.A. DATA, IngWare GmbH Bauinformatik, Erlenbach, Germany.

[34] DIANA FEA (2020) "Finite Element Analysis: User's Manual", Release 10.4. Delftechpark 19a, Delft, The Netherlands.

[35] TNO DIANA (2011) "Finite Element Analysis: User's Manual", Release 9.4.4. Delftechpark 19a, Delft, The Netherlands.

[36] L. MICCOLI, A. GAROFANO, P. FONTANA, U. MÜLLER (2015) Experimental testing and finite element modelling of earth block masonry. *Engineering Structures* **104** 80-94.

[37] R. KLEIN (1989) "Concrete and Abstract Voronoi diagrams. Lecture Notes in Computer Science" **200** Springer-Verlag, Berlin.

[38] UDEC (2011) "Version 4.01 – User's Guide". Itasca Consulting Group, Inc., Minneapolis, USA.

[39] J. MILOSEVIC, M. LOPES, A.S. GAGO, R. BENTO (2013) Testing and modeling the diagonal tension strength of rubble stone masonry panels. *Engineering Structures* **52** 581-591.

[40] G. VASCONCELOS, P.B. LOURENO (2009) Experimental characterization of stone masonry in shear and compression. *Construction and Building Materials* **23**(11) 3337-3345.

[41] J. MILOSEVIC, M. LOPES, A.S. GAGO, R. BENTO (2015) In-plane seismic response of rubble stone masonry specimens by means of static cyclic tests. *Construction and Building Materials* **82** 9-19.

[42] B. SILVA, J.M. GUEDES, A. ARDE (2012). Calibration and application of a continuum damage model on the simulation of stone masonry structures: Gondar church as a case study. *Bulletin Earthquake Engineering* **10** 211-234.

[43] E. VINTZILEOU (2014) Testing historic masonry elements and/or building models. In: A. Ansal (ed) "Perspectives on European Earthquake Engineering and Seismology. Geotechnical, Geological and Earthquake Engineering" **34**, Springer, Cham, Switzerland.